Journal of King Saud University – Science 35 (2023) 102681

HOSTED BY

Contents lists available at ScienceDirect

Journal of King Saud University – Science

journal homepage: www.sciencedirect.com

Original article

High performance of coating hydroxyapatite layer on 316L stainless steel using ultrasonically and alkaline pretreatment

Ahmad Fadli [a,*], Agung Prabowo [a], Silvia Reni Yenti [a], Feblil Huda [b], Ayla Annisa Liswani [a], Donda Lamsinar Br Hutauruk [a]

[a] Department of Chemical Engineering, Faculty of Engineering, Universitas Riau, Jl. H.R. Soebrantras, Km. 12.5, Pekanbaru, 28293, Riau, Indonesia
[b] Department of Mechanical Engineering, Faculty of Engineering, Universitas Riau, Jl. H.R. Soebrantras, Km. 12.5, Pekanbaru, 28293, Riau, Indonesia

ARTICLE INFO

Article history:
Received 12 September 2022
Revised 8 February 2023
Accepted 5 April 2023
Available online 13 April 2023

Keywords:
Pretreatment
Dip Coating
Hydroxyapatite
Coating Strength
Stainless Steel

ABSTRACT

One of the metals used for bone implants is 316L Stainless Steel, which is succesfully coated with hydroxyapatite to increase its low biocompatibility. Therefore, this study aims to carry out sonication, alkali, and heating treatment on 316L Stainless Steel substrates, determine the effect of temperature (A) sonication time (B), acetone concentration (C), bidirectional interaction of sonication temperature and time (AB), bidirectional interaction of sonication time and acetone concentration (BC), bidirectional interaction of sonication temperature and acetone concentration (AC) and the three-way interaction of sonication temperature, time and acetone concentration (ABC), a suitable empirical model for the coating process, and concentration of cleaning solution on the bond strength of the hydroxyapatite layer. The empirical model of the bond strength of the hydroxyapatite layer used was y = 426.1 – 11.50A – 19.25B – 6.229C + 0.6505AB + 0.1944AC + 0.2737 BCE – 0.00933 ABC with an R^2 value of 99.49%. The result showed that the layer's bond strength increases with the sonication temperature. It also showed that the longer the sonication time and the acetone concentration, the lower the bond strength value. The highest hydroxyapatite bond strength was produced at a sonication temperature, time, acetone concentration volume and bond strength of 45 °C, 15 min, 99%, and 91.35 Mpa, respectively.

1. Introduction

Fractures are the most common injuries caused as a result of accidents, and this tends to lead to osteoporosis in some circumstances. Its rate of occurrence is a global health issue, particularly in Indonesia. However, a creative way of handling this issue is through the availability of bone implants (Fadli et al., 2018). 316L Stainless Steel is one of the most frequently used materials. It consists of Cr (chromium), Ni (Nickel), Mo (Molybdenum), and low C (Carbon) content, making this material more robust than steel (Yuan et al., 2009, Kannan., 2004, Gray & Strong., 2009, Park et al., 2017). In addition, stainless steel is an iron compound that contains at least 10.5% Cr to prevent corrosive processes (Rasheed et al., 2016, Finsgar et al., 2016). This composition forms a protective layer due to the spontaneous oxidation of oxygen to chrome (Maver et al., 2020).

Osteoconductive biomaterials are frequently coated with osteoconductive biomaterials to ensure the clinical durability of metal implants. Hydroxyapatite is one of the materials used for bioactive coating (Nguyen et al., 2020, Weiner & Wagner, 1998\). Its benefits as a coating material include excellent bioactivity and prolonged osteoconductivity. Due to its chemical structure, crystallographic composition, and mineralogy similarity, hydroxyapatite forms a chemical link between the surface of the biomedical implant and the natural bone. This aids to stimulate its growth, thereby enhancing the osseointegration of human bone tissues (Chozhanathmisra et al., 2019).

Several methods of coating HA onto these implants have been previously described. These included dip-coating (Fadli et al., 2018) plasma spraying (Yan et al., 2003, Ratha et al., 2021), sputtering process (Vladescu et al., 2016, Trujillo et al., 2012, Yang et al., 2005), electrochemical deposition (Asri et al., 2016, Wang et al., 2011, Parcharoen et al., 2014), and sol–gel [Asri et al.,

* Corresponding author at: Department of Chemical Engineering, Universitas Riau, Pekanbaru, 28293, Riau, Indonesia.
E-mail address: fadliunri@yahoo.com (A. Fadli).
Peer review under responsibility of King Saud University.

Production and hosting by Elsevier

https://doi.org/10.1016/j.jksus.2023.102681
1018-3647/

2016, Wang et al., 2008). Dip coating or dipping methods are often adopted for metal plating processes using hydroxyapatite because the process is easy and inexpensive. In the present study, this approach was used to apply hydroxyapatite on a 316L Stainless Steel substrate. Meanwhile, in biomedical applications, it is essential to consider coating bonding on the surface of metal components. Before the emergence of a hydroxyapatite layer, surface treatment was carried out to strengthen its adhesion to the substrate (Gunawarman et al., 2020, Yusoff et al., 2014). Surface activation and roughness were improved by using ultrasonic treatments. According to Tsybry and Vyalikov (2017), plastic deformation occurs on a metallic surface under the impact of ultrasonic cavitation in fluids. Cavitation is the occurrence wherein bubbles develop in a liquid as a result of a drop in the liquid's pressure. Due to the bubble wall's tight confinement, a pressure gradient forms when the bubble wall pulses radially close to the wall. As a result, during the compression step, micro-jets are created and the bubbles close to the walls are easily distorted research on the ultrasonic cavitation-induced damage's properties and a description of the material's surface. When the trial period reaches 4 min, the inflection point for surface roughness will become visible. Due to the impact of micro-jets and shock waves produced by the collapse of bubbles close to the wall, cavitation holes develop in the early phases of cavitation erosion, increasing the surface roughness. Surface preparation before developing a hydroxyapatite layer in NaOH provides active sites and facilitates the precipitation of this element (Coelho et al., 2020).Several studies have been carried out on hydroxyapatite coating on metal substrates. For example, Fadli et al. (2021) applied the dip coating method on hydroxyapatite slurry with variation grams. In the study, a constituent composition of hydroxyapatite in distilled water was used to coat 316L Stainless Steel. This material was cleaned by immersing the substrate in acetone and coated in accordance with dipping time variations. Moreover, the best layer thickness obtained is 154 μm. Fadli et al. (2022) also applied this method on 316L Stainless Steel with hydroxyapatite (HA) consisting of various hydroxyapatite additions of 8, 10, and 12 g and dipping time variations of 2, 6, and 10 s. This tends to affect the thickness of the HAp layer deposited on the metallic surface of the 316L Stainless Steel. The rise in dipping time increases the hydroxyapatite layer on stainless steel. The thickest layer is 65 μm for a 12 gr hydroxyapatite addition and a dipping time of 10 s. Its shear strength increases with hydroxyapatite addition and dipping time. Du et al. (2014) performed ultrasonic cleaning and alkaline treatments on Ti6Al4V substrates prior to surface activation carried out before HA coating. These treatments led to forming a hydrogel layer of sodium titanate on the surface of the substrate. It turned into a Ti-OH group during the deposition process, which tends to support hydroxyapatite formation. At the same time, this group also strengthened the chemical bond between the Ti6Al4V substrate and the hydroxyapatite layer, resulting in higher crystallinity of HA as the treatment time increases. Ding et al. (2015) applied hydroxyapatite coating on a zinc-substituted titanium substrate (ZnHAp) with sonication in an ultrasonic cleaner. It was further followed by an alkaline pretreatment before the HA formation was realized by immersing the titanium plate in NaOH solution. A titanium oxide gel layer with Na + ions was formed on its surface, which increased the bond strength between HA and ZnHAp substrate. The NaOH treatment significantly increased the osseointegration of the electrochemically prepared HA on the substrate.Several previous studies on hydroxyapatite coating (Fadli et al.,2021, Fadli et al.,2022, Du et al., 2014, Ding et al.,2015) provided opportunities for future analysis. This aimed to develop a coating method to realize a better result in the bonding strength between hydroxyapatite and the substrate used for the bone implant. In this study, hydroxyapatite was coated on the 316L Stainless Steel using the dip approach, where the surface treatment was carried out before the formation of the layer on the substrate. Previous studies focused on the alkaline treatment, HA slurry composition, and the coating method. However, this study focused on ultrasonic treatment, which resulted in uniform roughness and improved surface activation. It also investigated the appropriate temperature and time for ultrasonic cleaning to yield the best result. This was followed by the alkaline treatment, which increases the adhesion of the coating to the substrate. This present study combined both ultrasonic and alkaline pretreatments to determine the bonding strength between HA and metal substrates. The results provided can be useful for future reference. The adhesive strength produced by the hydroxyapatite layer was compiled based on the regression model of the statistical analysis to identify the most influential variables.

However, by limiting the number of possible treatments, a factorial design is used to identify the factors that impact the response (Montgomery et al., 2013). The two-factor experiment, known as the simplest factorial design, only utilizes two independent variables. According to Borkowskiet al. (2015), it is an experimental design in which data are collected for all possible combinations of the two factors desired. The 2^{k} factorial design comprises k factors with low (-1) and high (+1) levels for each. The number of components (k) and multiplicity of levels (2) are written as a square and base number, respectively.

2. Experimental material and method

2.1. Substrate preparation

The 316L Stainless Steel was cut into the following sizes 3 cm × 2 cm × 0.1 cm (Jindal Stainless, India) as shown as Fig. 1and abraded in series with 1200 SiC paper. The sanded stainless steel was then ultrasonically washed with acetone. This is based on the predetermined sonication temperature, time, and concentration of acetone solution (Fuchs., 2015 and Skorb et al., 2010). Subsequently, alkali treatment was performed by soaking these substrates in 100 ml of 5 M NaOH aqueous solution at 60 °C for 24 h (Ding et al., 2015). The substrates were gently washed with distilled water and dried at 40 °C for 24 h in an oven. The alkali-treated substrates were then heated to 600 °C at a rate of 2 °C/min in a furnace (Lin et al, 2002). Finally, it was kept at a constant temperature for 1 h and cooled at room temperature.

2.2. Hydroxyapatite coating process

The coating slurry was prepared by mixing 12 gr of hydroxyapatite powder (Lianyungan Kede Chemical Industry co.Ltd, China)

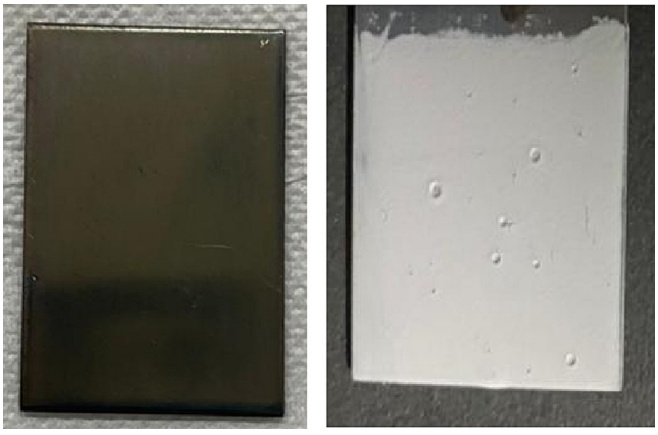

Fig. 1. Stainless Steel dimension before and after coated with hydroxyapatite.

into 24 ml of distilled water and 1 gr of polyethylene glycol. The suspension was then stirred with a magnetic stirrer at a speed of 400 rpm for 20 h. The dip coating apparatus is connected to the sterile stainless steel. The beaker containing the suspension is put underneath the apparatus. The substrate is further submerged into the suspension to start the immersion process, after which the device is turned off and left for 50 s. Finally, hydroxyapatite-coated substrates is heated to 110 °C in an oven for 10 min and sintered at a temperatures of 750 °C for 1 h at a heating rate of 2 °C/min (Fadli et al., 2021).

2.3. Coating characterisation

1. X-ray diffraction (XRD)

XRD was used to characterize the phase composition of an oxide layer and hydroxyapatite coating using Panalytical XRD XPERT POWDER operating from 10 to 90° 2θ at a step size of 0.026 2θ with CuKa radiation (Kα = 0.15406 nm) at 30 mA and 40 kV.

2. Scanning electron microscope (SEM)

The surface morphology of the formed hydroxyapatite coating and its thickness on the substrates was examined using a scanning electron microscope (SEM) Hitachi-SU 3500 and equipped with an energy dispersive X-ray spectrometer attachment. . . Bond strength analysis aims to determine the adhesiveness of the hydroxyapatite layer to the stainless steel metal.

2.4. Statistical analysis

Fractional design 2^{k} was used to select factors that influenced the mechanical properties of hydroxyapatite layers. This DOE design was carried out using Minitab 19 (Minitab Inc. USA). The three numerical variables include sonication temperature (A), sonication time (B), and acetone concentration (C). Table 1 shows the range of independent variables and experimental design levels used.

3. Result and discussion

3.1. Layer bond strength analysis

One of the requirements for the coating process is that the 316L Stainless Steel substrate and hydroxyapatite must form a strong layer bond. A shear test was carried out on this material coated with hydroxyapatite of the same metal size. The aim was to confirm the bond strength of the hydroxyapatite layer. This analysis was driven by the load required to remove the coating layer from the substrate (Moloodi et al., 2021, Mohseni et al., 2014).

Fig. 2 shows the enhanced bond strength between hydroxyapatite layers and the substrates. This was due to the variations in sonication temperature at each stage of the cleaning cycle and the acetone concentration. The bond strength increased from 36.64 MPa to 91.35 MPa when the sonication temperature was raised from 30^{0}C to 45^{0}C. This was due to a change in viscosity caused by a higher temperature. The low viscosity of the fluid due to the heating effect leads to the easy occurrence of cavitation. This is because the saturated vapor pressure of the fluid is higher, thereby causing its formation phase to be faster. Additionally, the increased sonication temperature lowers the cleaning solution's surface tension, making it easier for the fluid to break apart and enhancing cavitation intensity (Fuchs, 2015).

The maximum bond strength obtained without ultrasonication process in previous studied by Fadli et al, (2022) is 244 kPa. The binding strength of the hydroxyapatite layer is influenced by the sonication time. Incidentally, sonication was carried out for 15 to 30 min in this present study. In the bond strength of the acquired layer reduces as the sonication time increases. At 15 min, the layer's bond strength was measured to be 50.81 MPa, while at 30 min, it was 48.51 MPa. The ultrasonic treatment time tends to affect the coating strength value based on the roughness of the metal. The intensity of the plastic deformation, which occurs on the metal surface as the sonication period increases, is influenced by the material's structure. This increases the metal's roughness, although, it is reduced by sonication that goes on for very long (Tsybry &Vyalikov, 2017). According to Skorb et al., (2010), the roughness tends to decrease after 30 min of sonication because the surface has undergone a geometric shift caused by the production of erosive holes, accompanied by an increase in mass loss.

As the acetone concentration in the cleaning solution increases, the bond strength of the resultant hydroxyapatite layer diminishes,. Meanwhile, at a concentration of 70% by volume, the bond strength of the hydroxyapatite layer is 48.51 MPa, where at 99%, it is 31.73 MPa. At an acetone concentration of 99% by volume, the viscosity is lower than 70%. This causes cavitation since its vapor formation phase is accelerating. In addition, low viscosity promotes smaller surface tension which causes the fluid to break more easily and encourages greater cavitation intensity (Fuchs., 2015, Mason., 2016).

Due to the interaction effect of the three sonication parameters, it can be said that the ideal conditions in this study were at a sonication temperature of 45 ^{0}C, a sonication period of 15 min, and an acetone concentration of 99%. This is evident from the bond strength results at the same temperature and concentration, where the cavitation intensity is high at 45 °C and 99% acetone concentration, but at 30 min of continuous sonication, the cavitation intensity results in a change in surface geometry due to the formation of erosion pits and is accompanied by an increase in mass loss.

3.2. Diffractometry X-ray analysis

Fig. 3 shows the XRD surface pattern of a 316L Stainless Steel substrate after it had been subjected to alkali treatment by being submerged in a 10 M NaOH solution for 24 h and heated from 60 °C to 600 °C. When viewed on a diffractogram, sodium chromium oxide (Na_4CrO_4) compounds had patterns similar to the normal Na_4CrO_4 based on ICDD (International Centre of Diffraction Data). This is in accordance with Lin et al. (2002) that alkaline treatment and heating produce a layer of chromium oxide referred to as an inter-compound, usually formed alongside a covalent bond between 316L Stainless Steel metal and hydroxyapatite.

However, another phase was formed besides Na4CrO4, namely the sodium chromate (Na2CrO4). This compound was formed due to the chemical reaction between chromite or iron chromium oxide

Table 1
Coating Parameters Used In 2^{3} Factorial Design.

Parameter	Satuan	Level (*uncoded*)		Level (*coded*)	
Sonication Temperature (A)	°C	30	45	−1	+ 1
Sonication Time (B)	Minute	15	30	−1	+ 1
Acetone Concentration (C)	%Volume	70	99	−1	+ 1

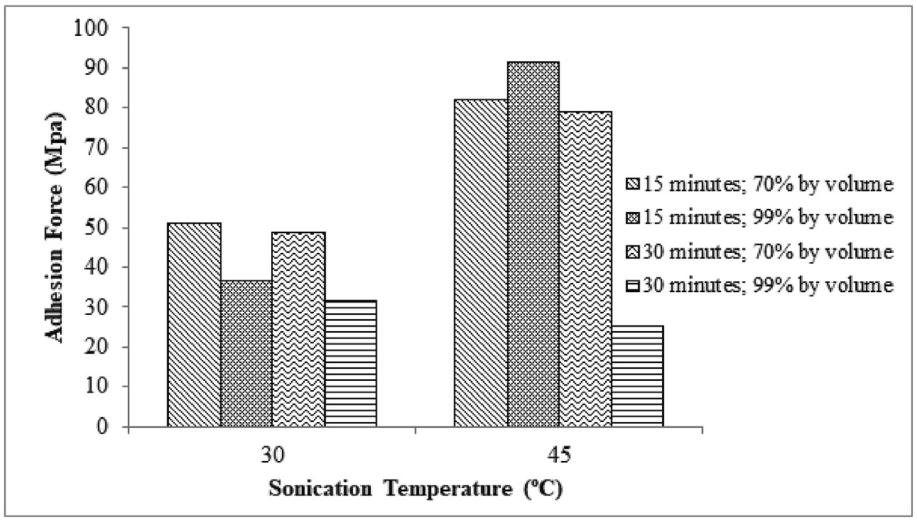

Fig. 2. The relationship between the bond strength of the Hydroxyapatite layer and the sonication temperature.

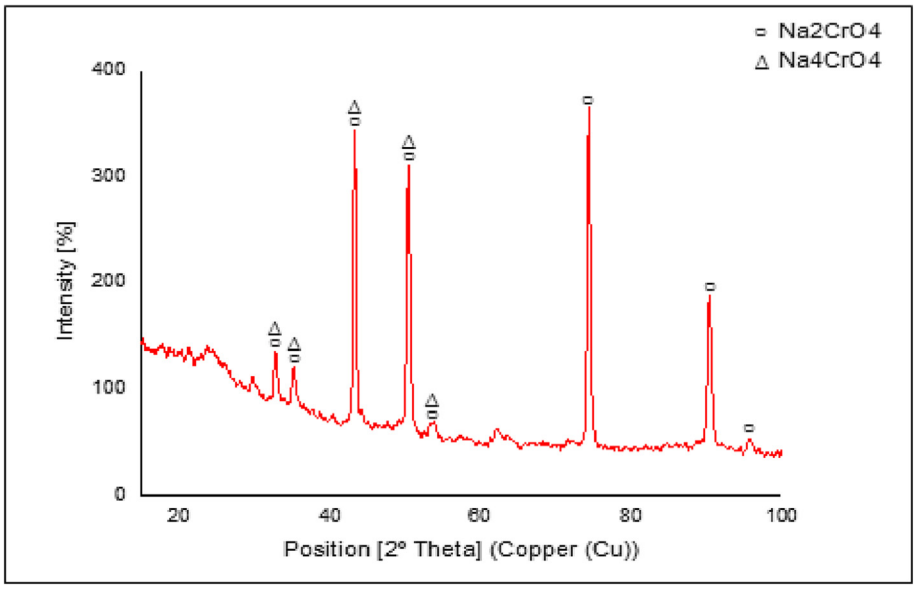

Fig. 3. Stainless steel 316L substrate after alkali treatment and heat treatment ICDD No. 01–078- 1507.

(FeCr2O4) and oxygen (Parirenyatwa et al., 2016). Fig. 4 shows the hydroxyapatite-coated substrates' XRD pattern. The primary diffraction peaks were detected at 2θ values of 25.6°, 31.4°, 32.5°, and 49.2°. These generally match the typical ICDD pattern of regular hydroxyapatite. The majority of its particles crystallize on the surface of the substrate, as proven by the high intensity of the diffractogram and the narrow breadth of the apex. The degree of kristanility obtained was 84.25%, therefore, it met the standard value, usually between 60 and 90%. A high degree of kristanility increases the adhesion of the hydroxyapatite layer (Hikmawati & Yasin., 2017).

3.3. SEM analysis

SEM analysis consists of four samples, which were used to discern the effect of sonication temperature, time, and acetone concentration on the thickness of the hydroxyapatite layer produced on the surface of the 316L Stainless Steel. The variations of sonication temperature and time, as well as acetone concentration of the four samples are (a) 45°C, 30 min, 99%; (b) 45°C, 15 min, 99%; (c) 45°C, 15 min, 70%; and (d) 30°C, 15 min, 99%. The average thickness of hydroxyapatite for the four samples was calculated as shown in Fig. 5. At a sonication temperature and time of 30 °C, and 15 min as well as an acetone concentration of 99% by volume, the average thickness of hydroxyapatite obtained was 44.49 μm. However, it was increased to 96.76 μm at a sonication temperature of 45 °C with the same time and acetone concentration.

The gluing of the hydroxyapatite layer on a stainless steel metal is also affected by alkaline pretreatment (NaOH) and heat. This forms a metallic-OH layer, and sodium chromate (Na_2CrO_4) compounds after the metal is sintered or treated. It functions as an inter-compound that increases the adhesion of hydroxyapatite to the substrate (Ding et al., 2015). The SEM result depicting the morphology of the metal surface is shown in Fig. 6, where the apatite formed is covered in small crystals.

The hydroxyapatite layer's standard thickness is 50 to 200 μm (Heiman, 2002). Samples b and c with a thickness of 96.76 μm met these requirements at sonication temperature, time and con-

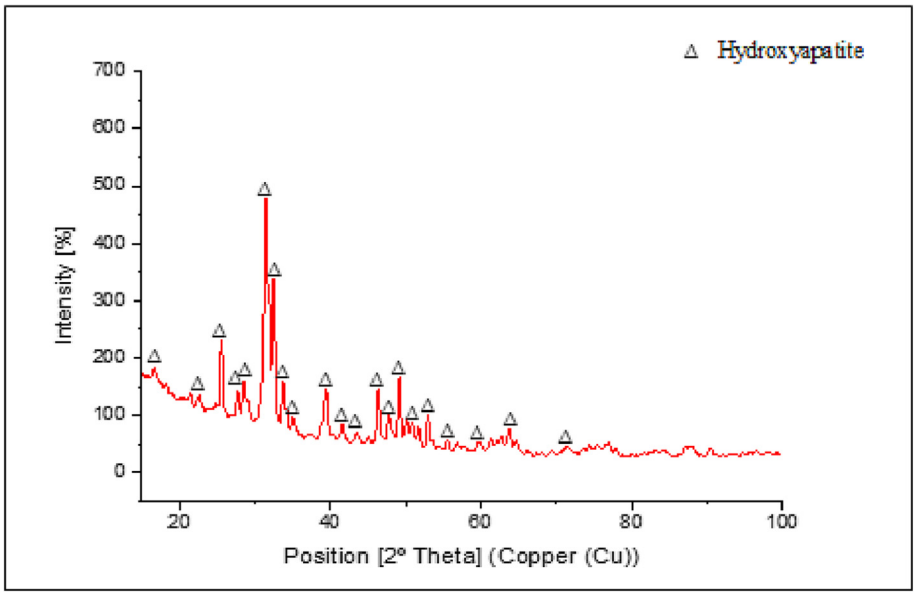

Fig. 4. Stainless steel 316L Substrate Diffractogram After Coating Hydroxyapatite ICDD No. 01–072-1243.

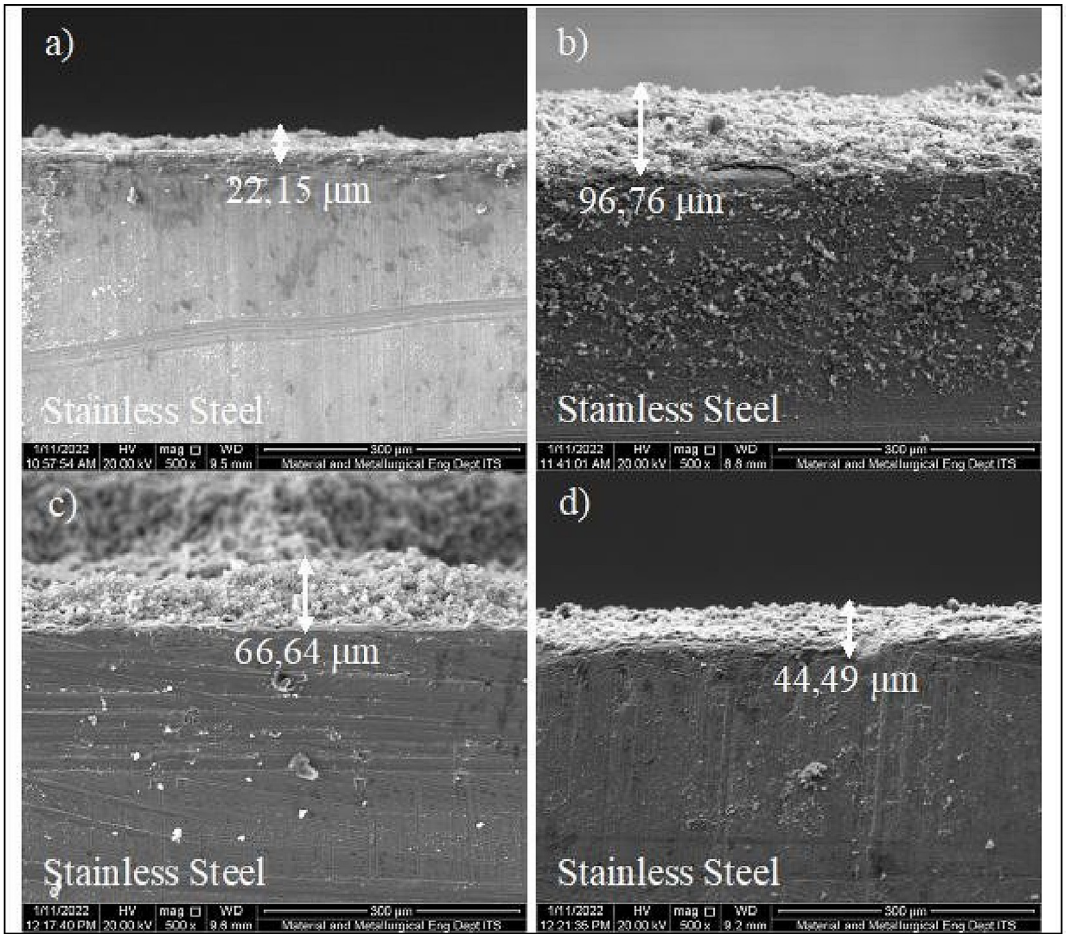

Fig. 5. Results of SEM Analysis of Hydroxyapatite Layer Thickness on 316L Stainless Steel with sonication temperature, sonication time, and acetone concentration variables, respectively (a) 45° C, 30 min, 99%; (b) 45° C, 15 min, 99%; (c) 45° C, 15 min, 70%; (d) 30° C, 15 min, 99%.

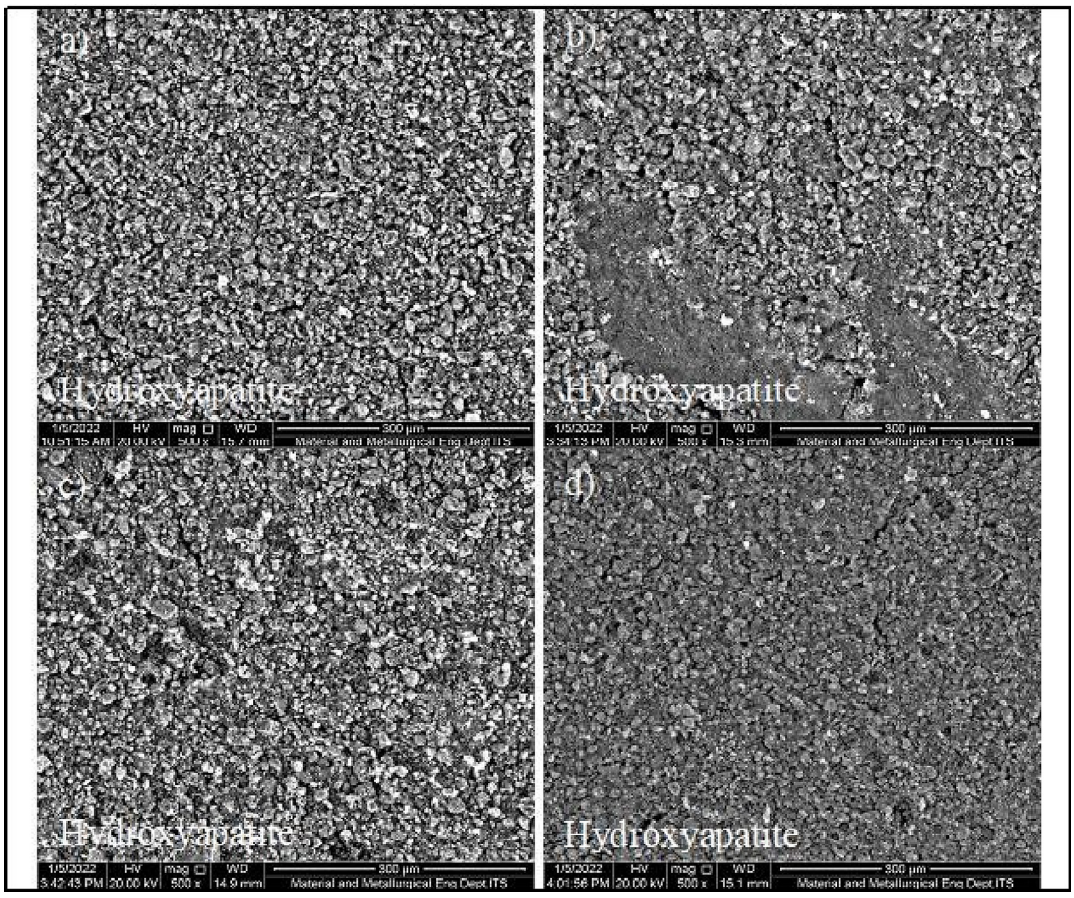

Fig. 6. Surface morphology of 316L stainless steel that has been coated with hydroxyapatite with sonication temperature, sonication time, and acetone concentration variables, respectively (a) 45^0 C, 30 min, 99%; (b) 45^0 C, 15 min, 99%; (c) 45^0 C, 15 min, 70%; (d) 30^0 C, 15 min, 99%.

centration of 45 °C, 15 min, and 99% volume. Meanwhile at 66.64 m, the sonication temperature, time and acetone concentration by volume were 45 °C, 15 min, and 70%, respectively.

3.4. Bonding strength model of HA coating on 316L stainless steel surface

The bond strength of the hydroxyapatite layer on the surface of 316L stainless steel was determined to obtain an empirical model using the dip coating method. The parameters and levels used in this study are summarized in Table 1.

Table 2 shows that the P-Value for all treatments was significant at 0.05, and when it is below 0.05, the parameter becomes less significant 0.05. Conversely, when it exceeds the significant degree, the factor or parameter affects the response (Montgomery., 2012).

The positive sign on the coefficient of sonication temperature effect (A) in the model indicates that the greater the parameter, the higher the bond strength of the layer obtained. The negative sign on the effective coefficient of sonication time (B), acetone concentration (C), bidirectional interaction of sonication temperature and time (AB), bidirectional interaction of sonication time and acetone concentration (BC), bidirectional interaction of sonication temperature and acetone concentration (AC) and the three-way interaction of sonication temperature, time and acetone concentration (ABC) in the model show that the increase in each parameter results in a decrease in the bond strength of the layer obtained.

Table 2
Statistical Analysis Results Using Minitab 2019.

Term	*Effect*	*Coef*	*P-Value*
Constant		55.62	0.133
A	27.39	13.70	0.078
B	−19.071	−9.535	0.111
C	−18.840	−9.420	0.112
AB	−15.464	−7.732	0.128
BC	−16.522	−8.261	0.136
ABC	−15.212	−7.606	0.139

R^2 = 99,49%; * The significance level is more than 0,05.

The model's suitability can be evaluated using the coefficient of determination (R^2). It is the variability in the data obtained or calculated based on the regression model. The value of R^2 provides a correlation between the experimental and predicted responses. According to Hasniyati et al. (2015), it is an evaluation of criteria where the value evaluates the correctness of the model. This must be high to enable the model to become significant. In other words, the R^2 value that is approximately 100% indicates a high degree of correlation between the observations made and the resulting model (Hasniyati et al., 2015). From the 2^3 factorial design modeling, the R^2 value obtained is 99.49%. It indicates that the model has a good fit and 99.49% of the parameters are explainable.

Figure 7 is a Pareto graph that states the parameters' significance on the hydroxyapatite layer's bond strength. Based on the diagram, it is evident that the variables that give the greatest to the smallest influence are sonication temperature (A), sonication time (B), acetone concentration (C), two-way interaction of sonication time and acetone concentration (BC), two-way interaction of sonication temperature and sonication time (AB), three-way interaction of sonication temperature, sonication time and acetone

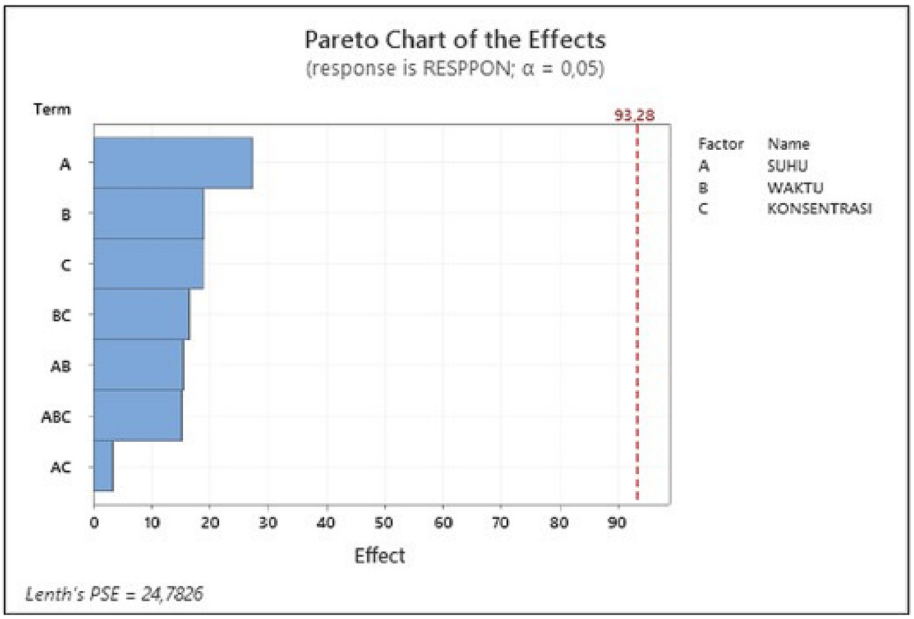

Fig. 7. Pareto Diagram in Modeling Bonding Strength of HA Layers.

concentration (ABC), two-way interaction of sonication temperature and acetone concentration (AC). Empirically, the bond strength of the hydroxyapatite layer based on the regression model from the results of statistical analysis is shown in the following equation.

$$y = 426.1 - - 11.50A - -19.25B - - 6.229C + 0.6505AB + 0.1944AC + 0.2737BCE - - 0.00933ABC$$

The predicted value of the bond strength of the hydroxyapatite layer can be calculated using the equation. The value of the bond strength based on predictions is shown in Table 3. The bond strength of the hydroxyapatite layer between the experimental results and the model has a small difference. Therefore, the bond strength of the predicted hydroxyapatite layer based on experiments can be plotted to determine the compatibility of the two values.

From the analysis of the statistical tests carried out, the model obtained is suitable for studying the effect of sonication temperature and time, including acetone concentration, on the hydroxyapatite layer bond strength response variables. The empirical model obtained significantly predicts the bond strength of the hydroxyapatite layer and can be analyzed by regression. This is evidenced by the predicted R^2 value obtained from the analysis of variance (ANOVA).

Table 3
Comparison of HA Layer Bonding Strength Values Based on Experimental Results and Model Predictions.

	Trial Experiment	Hydroxyapatite Bonding Strength (Mpa) Model
1	79.017	79.068
2	31.725	31.6894
3	81.818	81.999
4	48.510	48.492
5	50.807	50.901
6	25.079	25.1251
7	91.348	91.55305
8	36.641	36.7432

4. Conclusion

316L Stainless Steel was successfully coated with hydroxyapatite by performing sonication, alkali, and heating treatment on the substrate surface. The bond strength of the highest hydroxyapatite layer on the 316L Stainless Steel surface was 91.348 Mpa. The maximum hydroxyapatite layer thickness of 96.76 μm was obtained at a sonication temperature, time and acetone concentration of 45 °C, 15 min, and 99%. In addition, the empirical model used to control the bond strength of the hydroxyapatite layer during the coating process on the 316L Stainless Steel surface is y = 426.1 – 11.50A– 19.25B – 6.229C + 0.6505AB + 0.1944AC + 0.2737 BCE – 0.00933 ABC, where the R^2 obtained for this model is 99.49%.

Declaration of Competing Interest

The authors declare that they have no known competing financial interests or personal relationships that could have appeared to influence the work reported in this paper.

Appendix A. Supplementary material

Supplementary data to this article can be found online at https://doi.org/10.1016/j.jksus.2023.102681.

References

Asri, R.I.M., Harun, W.S.W., Hassan, M.A., Ghani, S.A.C., Buyong, Z., 2016. A review of hydroxyapatite-based coating techniques: sol–gel and electrochemical depositions on biocompatible metals. J. Mech. Behav. Biomed. Mater. 57, 95–108.

Borkowski, J., Ward, N., Otto, J., Swinford, S., 2015. Measuring Minnesota's Traffic Safety Culture. Montana State University, Bozeman.

Chozhanathmisra, M., Pandian, K., Govindaraj, D., Karthikeyan, P., Mitu, L., Rajavel, R., 2019. Halloysite nanotube-reinforced ion-incorporated hydroxyapatite-chitosan composite *coating* on Ti-6Al-4 V alloy for implant application. J. Chem. 2019, 1–12. https://doi.org/10.1155/2019/7472058.

Coelho, M.F., De Sousa, L.L., Ferreira, C.C., De Souza, B.F., Da Silva Rigo, E.C., Mariano, N.A., 2020. Biomimetic *coating* on titanium: evaluation of bioactivity and corrosion. Mater. Res. Express 6, 1265g5. https://doi.org/10.1088/2053-1591/ab67f1.

Ding, Q., Zhang., Huang, Y., Yan., Pang, X., 2015. In Vitro Cytocompatibility And Corrosion Resistance Of Zinc-Doped Hydroxyapatite *Coatings* On A Titanium

Substrate. Journal Of Materials Science. 50, 189-202. https://doi.org/10.1007/s10853-014-8578-4
Du, J., Liu, X., He, D., Liu, P., Ma, F., Li, Q., Feng, N., 2014. Influence Of Alkali treatment on Ti6Al4V alloy and the HA *coating* deposited by hydrothermal-electrochemical methods. Rare Metal Mater. Eng. 43, 830–835. https://doi.org/10.1016/S1875- 5372(14)60093-X.
Fadli, A., Akbar, F., Prabowo, A., Hidayah, P.H., 2018. Coating hydroxiapatite on stainless steel 316 L by using Sago starch as binder with dip-coating method. IOP Conf. Ser.: Mater. Sci. Eng. 345,. https://doi.org/10.1088/1757- 899X/345/1/012036 012036.
Fadli, A., Yenti, S.R., Huda, F., Prabowo, A., Marbun, U.N., 2021. Empirical model to predict the hydroxyapatite thickness on the surface of 316L stainless steel by the dip coating method. Ceram.-Silikáty 65, 386–394. https://doi.org/10.13168/cs.2021.0041.
Fadli, A., Mulya, N., Pane, K.B., Pratama, A., 2022. Effect of solid loading and dipping time on microstructure and shear strength of hydroxyapatite coatings deposited via dip coating technique. IOP Conf. Ser.: Earth Environ. Sci. 963,. https://doi.org/10.1088/1755-1315/963/1/012019 012019.
Finšgar, M., Uzunalić, A.P., Stergar, J., Gradišnik, L., Maver, U., 2016. Novel chitosan/diclofenac coatings on medical grade stainless steel for hip replacement applications. Sci. Rep. 6 (1), 26653.
Fuchs, F.J., 2015. Ultrasonic cleaning and washing of surfaces. Power Ultrason. 2015, 577–609. https://doi.org/10.1016/B978-1-78242-028-6.00019-3.
Gray-Munro, J.E. and Strong, M., 2009. The mechanism of deposition of calcium phosphate coatings from solution onto magnesium alloy AZ31. *Journal of Biomedical Materials Research Part A: An Official Journal of The Society for Biomaterials, The Japanese Society for Biomaterials, and The Australian Society for Biomaterials and the Korean Society for Biomaterials*, *90*(2), pp.339-350. https://doi.org/10.1002/jbm.a.32107
Gunawarman, G., Affi, J., Sutanto, A., Putri, D.M., Juliadmi, D., Nuswantoro, N.F., Manjas, M., 2020. Adhesion strength of hydroxyapatite coating on titanium materials (Ti-6Al-4V ELI) for biomedical application. Mesin 11, 1–7. https://doi.org/10.25105/ms.v11i2.7448.
Hasniyati, M. R., Zuhailawati, H., Ramakrishnan, S., Dhindaw, B. K., Mohd Noor, S. N. F., 2015. Design Of Experiment DOE Study Of Hydroxyapatite-Coated Magnesium By Cold Spray Deposition. Materials Science Forum. 819, 341-346. https://doi.org/10.4028/www.scientific.net/MSF.819.341.
Heimann, R.B., 2002. Materials science of crystalline bioceramics: a review of basic properties and applications. Chiang Mai Univ. J. 11, 1–23.
Hikmawati, D., Yasin, M., 2017. The effect of sintering temperature to the quality of hydroxyapatite coating on cobalt alloys as the candidate of bone implant prosthesis. J. Biomimet., Biomater. Biomed. Eng. 321, 59–68. https://doi.org/10.4028/www.scientific.net/JBBBE.32.59.
Kannan, S., Balamurugan, A., Rajeswari, S., 2004. H2SO4 as a passivating medium on the localised corrosion resistance of surgical 316L SS metallic implant and its effect on hydroxyapatite coatings. Electrochim. Acta 49 (15), 2395–2403. https://doi.org/10.1016/j.electacta.2004.01.003.
Lin, F.H., Hsu, Y.S., Lin, S.H., Sun, J.S., 2002. The effect Of Ca/P concentration and temperature of simulated body fluid on the growth of hydroxyapatite coating on alkali- treated 316L stainless steel. Biomaterials 2319, 4029–4038. https://doi.org/10.1016/S0142-9612(02)00154-0.
Mason, T.J., 2016. Ultrasonic cleaning: an historical perspective. Ultrason. Sonochem. 29, 519–523. https://doi.org/10.1016/j.ultsonch.2015.05.004.
Maver, U., Xhanari, K., Zizek, M., Gradisnik, L., Repnik, K., Potocnik, U., Finsgar, M., 2020. Carboxymethyl cellulose/diclofenac bioactive coatings on AISI 316LVM for controlled drug delivery, and improved osteogenic potential. Carbohydr. Polym. 230,. https://doi.org/10.1016/j.carbpol.2019.115612 115612.
Mohseni, E., Zalnezhad, E., Bushroa, A.R., 2014. Comparative investigation on the adhesion of hydroxyapatite coating on Ti–6Al–4V implant: a review paper. Int. J. Adhes. Adhes. 48, 238–257. https://doi.org/10.1016/j.ijadhadh.2013.09.030.
Moloodi, A., Toraby, H., Kahrobaee, S., Razavi, M.K., Salehi, A., 2021. Evaluation of fluorohydroxyapatite/strontium coating on titanium implants fabricated by hydrothermal treatment. Prog. Biomater. 103, 1–9. https://doi.org/10.1007/s40204-021-00162-7.
Montgomery, D.C., 2012. Statistical Quality Control. Wiley Global Education, Arizona.
Montgomery, D.C., 2013. Design and Analysis of Experiments. John Wiley and Sons Inc, Arizona.
Nguyen, V.T., Cheng, T.C., Fang, T.H., Li, M.H., 2020. The fabrication and characteristics of hydroxyapatite film grown on titanium alloy Ti-6Al-4V by anodic treatment. J. Mater. Res. Technol. 93, 4817–4825. https://doi.org/10.1016/j.jmrt.2020.03.002.
Parcharoen, Y., Kajitvichyanukul, P., Sirivisoot, S., Termsuksawad, P., 2014. Hydroxyapatite electrodeposition on anodized titanium nanotubes for orthopedic applications. Appl. Surf. Sci. 311, 54–61. https://doi.org/10.1016/j.apsusc.2014.04.207.
Parirenyatwa, S., Escudero-Castejon, L., Sanchez-Segado, S., Hara, Y., Jha, A., 2016. Comparative study of alkali roasting and leaching of chromite ores and titaniferous minerals. Hydrometall. 165, 213–226. https://doi.org/10.1016/j.hydromet.2015.08.002.
Park, K.H., Kim, S.J., Hwang, M.J., Song, H.J., Park, Y.J., 2017. Pulse electrodeposition of hydroxyapatite/chitosan coatings on titanium substrate for dental implant. Colloid Polym. Sci. 295, 1843–1849. https://doi.org/10.1007/s00396-017-4166-x.
Rasheed, N.K., Hubeatir, K.A., Hmood, A.F., 2016. Improvement of corrosion resistance of dental alloys in oral environment at different temperature by laser irradiation. Australian J. Basic App. Sci. 10, 162–170.
Ratha, I., Datta, P., Balla, V.K., Nandi, S.K., Kundu, B., 2021. Effect of doping in hydroxyapatite as coating material on biomedical implants by plasma spraying method: a review. Ceram. Int. 47 (4), 4426–4445. https://doi.org/10.1016/j.ceramint.2020.10.112.
Skorb, E.V., Shchukin, D.G., Mohwald, H., Andreeva, D.V., 2010. Ultrasound-driven design of metal surface nanofoams. J. Nanoscale 25, 1–5. https://doi.org/10.1039/c0nr00074d.
Trujillo, N.A., Floreani, R., Ma, H., Bryers, J.D., Williams, J.D., Popat, K.C., 2012. Antibacterial effects of silver-doped hydroxyapatite thin films sputter deposited on titanium. Mater. Sci. Eng. C 32 (8), 2135–2144. https://doi.org/10.1016/j.msec.2012.05.012.
Tsybry, I.K., Vyalikov, I.L., 2017. Analysis of cavitation on the surface of steel under the ultrasonic cleaning. Mater. Sci. Eng. 1771, 1–6. https://doi.org/10.1088/1757-899X/177/1/012135.
Vladescu, A., Padmanabhan, S.C., Azem, F.A., Braic, M., Titorencu, I., Birlik, I., Morris, M.A., Braic, V., 2016. Mechanical properties and biocompatibility of the sputtered Ti doped hydroxyapatite. J. Mech. Behav. Biomed. Mater. 63, 314–325. https://doi.org/10.1016/j.jmbbm.2016.06.025.
Wang, D., Chen, C., He, T., Lei, T., 2008. Hydroxyapatite coating on Ti6Al4V alloy by a sol–gel method. J. Mater. Sci. - Mater. Med. 19, 2281–2286. https://doi.org/10.1007/s10856-007-3338-5.
Wang, L.N., Luo, J.L., 2011. Preparation of hydroxyapatite coating on CoCrMo implant using an effective electrochemically-assisted deposition pretreatment. Mater. Charact. 62 (11), 1076–1086.
Weiner, S., Wagner, H.D., 1998. The material bone: structure-mechanical function relations. Annu. Rev. Mater. Sci. 28 (1), 271–298.
Yan, L., Leng, Y., Weng, L.T., 2003. Characterization of chemical inhomogeneity in plasma-sprayed hydroxyapatite coatings. Biomaterials 24 (15), 2585–2592. https://doi.org/10.1016/S0142-9612(03)00061-9.
Yang, Y., Kim, K.H., Ong, J.L., 2005. A review on calcium phosphate coatings produced using a sputtering process—an alternative to plasma spraying. Biomaterials 26 (3), 327–337. https://doi.org/10.1016/j.biomaterials.2004.02.029.
Yuan, Q., Sahu, L.K., D'Souza, N.A., Golden, T.D., 2009. Synthesis of hydroxyapatite coatings on metal substrates using a spincasting technique. Mater. Chem. Phys. 116 (2–3), 523–526. https://doi.org/10.1016/j.matchemphys.2009.04.027.
Yusoff, M.F.M., Kadir, M.R.A., Iqbal, N., Hassan, M.A., Hussain, R., 2014. Dipcoating of poly (ε-caprolactone)/hydroxyapatite composite coating on Ti6Al4V for enhanced corrosion protection. Surf. Coat. Technol. 245, 102–107. https://doi.org/10.1016/j.surfcoat.2014.02.048.